Rutherford Appleton Laboratory

RAL 86–078

An Intense Transmission Spectrometer for Isis

R J Newport and W S Howells
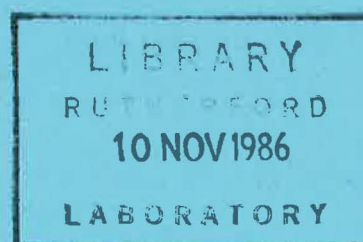
AN INTENSE TRANSMISSION SPECTROMETER FOR ISIS   RAL 86078

R J Newport* and W S Howells

Neutron Division
Rutherford Appleton Laboratory
Chilton
Didcot
Oxon   OX11 0QX

ABSTRACT

This report seeks to outline a design for an intense transmission
spectrometer (ITS) suitable for installation on the pulsed neutron source
ISIS. The performance of the instrument is evaluated and several examples
of the areas of science made accessible are discussed. It is shown that
the proposed design will represent a scientifically valuable and cost-
effective addition to the present suite of ISIS instruments.

July 1986

* Physics Laboratory, University of Kent, Canterbury, CT2 7NR.

CONTENTS

1. INTRODUCTION

One of the most basic of all neutron scattering studies is the determination of the total cross section as a function of energy, $\sigma(E)$ using transmittance measurements. The spectrometer and associated instrumentation required to carry out such measurements may be described as relatively simple, particularly when discussed in relation to pulsed neutron sources [1]. The detailed scientific and technological information that can be extracted from the $\sigma(E)$ covers, however a very wide range and may require the use of fairly elaborate data analysis techniques. This report seeks to describe the principles of a pulsed source transmission spectrometer, to suggest some of the areas of science and technology which may be able to exploit such an instrument, and to present an outline design and specification for a suitable spectrometer for ISIS.

2. TRANSMITTANCE MEASUREMENTS ON A PULSED NEUTRON SOURCE

a) Principles

The generic pulsed source transmission spectrometer is shown schematically in Figure 1. The ratio of transmitted neutron flux to incident flux is measured, in principle, using spectra acquired with the sample in the beam and then with the sample removed. In practice it will also be necessary to measure carefully the energy-dependant background using resonance absorption filters which are "black" to neutrons within some energy band (i.e. resonance absorbers that are thick enough to remove all incident neutrons in the region of the resonance peaks). The time-of-flight technique is used to provide energy or wavelength analysis:

$$E = \frac{m(L_i + L_f)^2}{2t^2} \qquad\qquad \lambda = \frac{ht}{m(L_i + L_f)} \qquad\qquad (1)$$

where t is the measured time-of-flight and L_i, L_f are the incident and final path lengths.

If, in any one time channel (i.e. at some corresponding value of E or λ) the counts recorded with the sample out of and in the beam are C_0 and C_1 respectively then the transmittance, and hence the cross section may be written:

$$\tau = C_1/C_0 \qquad\qquad \text{and,} \qquad \sigma = -\ln \tau/N \qquad\qquad (2)$$

where N is the number of sample nuclei in the beam. It is assumed that the sample completely covers the incident beam and that it has uniform thickness. The spectra from which C_0 and C_1 are drawn will have been normalised to their respective time-sorted monitor spectra. The normalisation must of course be performed using an energy or wavelength scale rather than a raw t-o-f scale. Measured in this way τ will not normally be dependant on variations in incident flux or, indeed on such instrumental parameters as detector efficiency.

The resolution is given by applying:

$$\Delta E = \left\{ \left(\frac{\partial E}{\partial L}\right)^2 \Delta L^2 + \left(\frac{\partial E}{\partial t}\right)^2 \Delta t^2 \right\}^{\frac{1}{2}}$$

to equation (1), yielding:

$$\Delta E/E = 2\Delta\lambda/\lambda = \left\{ \left(\frac{\Delta L}{L}\right)^2 + \left(\frac{2\Delta t}{t}\right)^2 \right\}^{\frac{1}{2}} \tag{3}$$

where Δt includes uncertainties due to the proton pulse width (0.4 µs), the moderator emission times and the width of the t-o-f channels at the detector; ΔL is the path length uncertainty. The sample-out intensity at the detector (counts per second per time channel, Δt_D) can be calculated from the following expression [1]:

$$I(E) = n(E) \, A_m A_D \eta_D(E) \cdot 2 \frac{(2E^3/m)^{\frac{1}{2}}}{(L_i + L_f)^3} \Delta t_D \tag{4}$$

where A_m and A_D are the moderator and detector areas respectively, $\eta_D(E)$ is the detector efficiency and $n(E)$ is the number of neutrons leaving the moderator face per unit area, solid angle, energy and time. The appropriate energy interval ΔE corresponding to the given detector time channel width Δt_D was obtained by differentiating equation (1):

$$\Delta E = -m \frac{(L_i + L_f)^2}{t^3} \Delta t_D = \left(\frac{2E^3}{m}\right)^{\frac{1}{2}} \frac{2}{(L_i + L_f)} \Delta t_D$$

The statistical error in the transmittance value is given by:

$$\frac{\delta\tau}{\tau} = \left(\frac{1}{C_0} + \frac{1}{C_1}\right)^{\frac{1}{2}} \tag{5}$$

and the corresponding statistical error in the total cross section is:

$$\frac{\delta\sigma}{\sigma} = -\frac{\delta\tau}{\tau \ln \tau} \tag{6}$$

Too small a sample will, therefore, give rise to a large fractional error. Likewise, if the sample attenuates the beam too much the error will be large; this situation may occur for example if the sample has

one or more nuclear resonance associated with it in the energy range of interest. It is also important to note that a resonant attenuator at any position in the beam will have the same effect.

The total error in the cross section may be written:

$$\Delta\sigma = \{(\frac{\partial\sigma}{\partial\tau})^2 \ \Delta\tau^2 + (\frac{\partial\sigma}{\partial N})^2 \ \Delta N^2\}^{\frac{1}{2}}$$

whence,

$$\frac{\Delta\sigma}{\sigma} = \{(\frac{\Delta\tau}{\tau\ln\tau})^2 + (\frac{\Delta N}{N})^2\}^{\frac{1}{2}} \tag{7}$$

It is likely that for most samples the dominant contribution to ΔN will arise from the uncertainty in sample thickness, rather than any uncertainty in the bulk atomic density.

In Section 4 these general principles will be applied to a proposed instrument for the spallation neutron source ISIS and it will be shown that an energy resolution of $\sim 0.3\%$, combined with a count rate per resolution element of $\sim 10^3 - 10^4$ per second is achievable.

b) Measurement of background

A major limitation to the measurement of accurate cross sections is the determination of the energy-dependant background, particularly for samples exhibiting regions of high beam attenuation. It is possible to determine the combined neutron plus γ-ray background using a series of beam filters having strong resonances with transmission for neutrons close to zero over several energy (or corresponding time) resolution widths (e.g. [2], [3]). To take account of the change in background due to the presence of the sample, the spectra must be recorded with and without the sample in the beam. The filters themselves attenuate the beam-borne background; by varying the filters' thicknesses however it is possible to extrapolate to a "zero thickness" value. Should it be necessary, the contribution to the background arising from γ-rays alone may be measured by placing a large polythene filter in the beam which will transmit γ-rays above

~ 1 MeV but which effectively removes neutrons of energies less than ~ 100 keV.

This "black" resonance technique only determines the level of the background in the region of each resonance energy and some interpolation scheme is therefore needed. The following forms for the background intensity as a function of the time-of-flight, t, have been used successfully in precision cross section determination using t-o-f method (e.g. [2]):

$$I_B(t) = \alpha + \beta\, t^{-\gamma} \exp(-\nu/t)$$

$$I_B(t) = \alpha + \beta/t + \gamma \exp(-\nu t) \tag{8}$$

The parameters α, β, γ and ν are obtained from a fit to the counts in the spectral minima associated with each "black" resonance. These background correction procedures, and the method as a whole, can be tested against a "standard" such as carbon which has a constant total cross section [4]. Consistency checks between each set of spectra are also useful indicators.

3. ITS: SCIENTIFIC AND TECHNOLOGICAL USES

There are many aspects to the potential usage of an intense transmission spectrometer, the more obvious or important of these are outlined below.

a) Cross sections for data analysis

In all neutron scattering experiments there will be multiple scattering and attenuation components to the data. The problems arising from these effects vary in magnitude and seriousness and may ·be ignored or accounted for within the data analysis process. In some cases however it is highly desirable to have an accurate measure of the sample's total cross section over the range of neutron energies used in the experiment. This may best be performed by a transmission experiment which uses the same, or comparable incident beam flux as that associated with main experiment. This was the principal use envisaged for a transmission spectrometer in the early deliberations on ISIS instrumentation [5]; the importance of such a facility at a pulsed neutron source remains (see, for example [6]).

b) Condensed matter studies

For most isotopes, the absorption cross section $\sigma_a(E)$ at energies below $\sim$ 1 eV is proportional to $E^{-\frac{1}{2}}$ [4,7]. It is possible therefore 'to obtain the total scattering cross section, $\sigma_s(E)$ from the measured total cross section, $\sigma(E)$. Moreover it is then possible to extract a radial distribution function from the distinct part of $\sigma_s(E)$ [1,8,9]; hence the experimental $\sigma(E)$ must be corrected for both absorption and incoherent scattering. Within the static approximation and for isotropic systems (for which the wave vector transfer, Q, is a function of scattering angle only, with maximum value $Q_{max} = 4\pi/\lambda = (8mE)^{\frac{1}{2}}/h$), the real-space correlation functions may be computed from the Fourier cosine transformation of $Q^2_{max} \sigma_{s,D}(Q_{max})$.

As an example of this technique, the total correlation function for SiO_2 glass obtained from a transmittance measurement is compared in Figure (2a) with that from a 2-axis diffractometer. Figure (2b) shows the corrected data for $\sigma(E)$. Whilst the transmittance-derived results are not as accurate as their conventional diffraction counterparts,

they do illustrate that the technique is capable of yielding useful structural information of reasonable quality. Potential applications include:

i) those experiments requiring a bulky sample containment and environment (e.g. at high pressures, and perhaps also at high temperatures).Multiple scattering corrections are negligible and container/environment absorption problems are essentially trivial.

ii) experiments requiring a high data acquisition rate (e.g. corrosive, chemically decaying, and very small samples or small portions of samples).

iii) experiments requiring exceptionally good statistics (e.g. thin films).

iv) feasibility studies prior to a diffraction experiment.

The method has also been applied to the study of defects in crystals [10], but such work requires only long wavelength neutrons well beyond the Bragg cut-off and is not suited to the instrument under consideration here.

c) **Bragg edge measurements**

As the wavelength of neutrons incident on a powder decreases to twice a crystal plane spacing, 2d, there will be a sharp decrease in measured transmittance associated with a rise in the cross section – this is the Bragg edge (transmission measurements are in this context analogous to diffraction with $2\theta = 180°$). The transmittance will then rise, until the condition $\lambda = 2d$ is again satisfied. It is possible therefore to obtain a fast, accurate determination of lattice parameters. The Bragg edges in the cross section for iron have been observed using a transmission spectrometer on a pulsed source [11]; some of the data is reproduced in Figure 3. The full data set extended to 0.95 eV, and strong features were evident up to $h^2+k^2+l^2 = 190$. Many of the applications suggested in the previous section could be repeated here. For experiments requiring very high resolution at energies below ~ 25 meV, a very long flight path instrument such as the HRPD on ISIS would be recommended. In this context it is also worth noting in advance of Section 4 that frame overlap for the instrument to be proposed by this report occurs at E = 4.5 meV.

d) Vibrational spectroscopy

The scattering cross section of an isotope decreases from its "bound" value at low energies to a "free" value at energies much greater than the binding energy of the system in which it is embedded. For an isotope of mass M the ratio of free to bound cross sections is $(M/(M+1))^2$. The effect is only significant therefore for low mass nuclei and, because of the large bound cross section for hydrogen, is of particular importance for the study of hydrogenous systems using "white" neutron beams. For a system with energy levels at $h\omega_0$, $h\omega_1$, ..., $\sigma(E)$ will fall to a minimum whenever the incident neutron energy equals one of the excitation energies [12]. The cusp-like minima in $\sigma(E)$ will be broadened by thermal motions, but this problem may be greatly reduced by cooling. Examples of the data from early studies using this method on room temperature metal hydrides [13] are reproduced in Figure 4. The theoretical curve plotted with the $ZrH_{1.5}$ data is based on an isotropic harmonic oscillator model [12]; using the fundamental frequency as a fitting parameter yields $h\omega_0 = 137$ meV. It is also evident that anisotropic effects are observed. Potential applications of high count rate, good resolution transmittance measurements in the field of vibrational spectroscopy include the study of corrosive samples, low-coverage surface systems or intercalates, deuterated systems and kinetic studies. Demand for such measurements is likely to be high [14].

e) Neutron-nuclear resonances

The accurate determination of neutron-nuclear resonance parameters in the epithermal region is a valuable pursuit in its own right as the data available for some isotopes is far from complete [4]. Given the availability of sophisticated multi-parameter, multi-level R-matrix fitting routines [15], it is possible to extract accurate and precise resonance information. The limitations on these cross section measurements depends largely on the energy resolution required; the instrument envisaged in this report could certainly yield useful information to $E \sim 20$ eV. For resonances having large values of Γ (the FWHM), the maximum useful energy would be even higher.

Beyond the determination of resonance parameters for their own sake, there have already been trial experiments to investigate one possible technological application as a non-invasive temperature probe [16]. The measured resonance interaction cross section has a width greater than Γ due to the effects of Doppler broadening [17]. To a first approximation the resonance cross section peak is depressed by $\Gamma/(\Gamma+\Delta)$ and the width is increased to $(\Gamma+\Delta)$, where the Doppler width Δ is given by

$$\Delta = (4m_n \, Ek_BT^*/M)^{\frac{1}{2}} \qquad ; \qquad T^* \simeq (3\theta_D/8) \coth (3\theta_D/8T)$$

θ_D is the Debye temperature, T is the thermodynamic temperature. A ratio of two transmission spectra centred on the 1.098 eV Hf-177 resonance and taken at T = 300K and T = 1010K is shown in Figure 5. The effect of Doppler broadening is clearly demonstrated. Combining data from this and other resonances exhibited by the metal alloy sample used in this test experiment, an accuracy of $\Delta T = \pm$ 5K in estimated temperatures was achieved. Careful fitting to a cross section measurement, with T as the principal variable, may give even better accuracy. The temperature value obtained in this way is the mean over the whole neutron path length of the particular isotope giving rise to the resonance (or series of resonances); it therefore corresponds to a bulk value. By coating several surfaces with thin layers of materials having suitable resonances, it may prove possible for example to measure the temperature distribution in a fairly bulky, complex piece of machinery [16].

f) "Test-bed" studies

If designed with sufficient flexibility (e.g a large, open sample and detector area), a transmission spectrometer could contribute to a wide range of short-term tests, trials and development studies. For example, during the development of a new detector assembly it is often necessary to have access to a neutron beam in order that performance, and progress can be monitored. It is also conceivable that novel experimental techniques and methods could be assessed.

4. ITS: DESIGN AND PERFORMANCE

a) Beamline layout

Given the existing pressure on the few remaining unallocated ISIS beams and the relatively lowly requirements of a transmission spectrometer, it is suggested that the instrument be sited downstream of LAD (the Liquids and Amorphous materials Diffractometer) on the S7 beamline. A general scheme for this symbiotic layout is shown in Figure 6; a diagramatic section through the beamline is shown in Figure 7. The existing LAD beamdump has been moved out towards the boundary of the experimental hall and replaced by an evacuated drift tube, leaving ample area for the proposed intense transmission spectrometer ITS. It may be worth pointing out at this stage that, although the "standard" LAD/ISIS beamdump is shown, it is highly unlikely that such a massive structure would be required in this context: a smaller beamdump would allow longer flight paths and improved resolution. The drift tubes will have their inner surfaces "broken up" by B_4C/resin "crispy mix" rings [18]; in the tube from LAD these should come outside the beam penumbra. Substantial wax/borax shield walls must be placed around the drift tube between LAD and ITS sample area. With these precautions it is felt that the background at LAD due to backscattering from the ITS sample will, at the worst, present no more of a problem than is tolerated from the existing beamdump. To ensure maximum flexibility it is suggested that the vacuum vessels for the sample, detector and drift tubes are sited on a simple plinth and be removable. The whole area would be enclosed within a blockhouse, bounded on either side by the common shielding walls with HRPD and MARS.

b) Beam definition

The design of the existing LAD incident beam collimation constrains much of our discussion on ITS. The final LAD collimator aperture is at 8.85 m from the CH_4 methane moderator and has maximum dimensions 26 x 32 mm (a reduction in area may occur, depending on LAD operating conditions but this merely reduces the ITS count rate). The LAD beam umbra has vanished, therefore by about 13 m. At the closest practicable sample position of L_1 = 14.5 m the sample will have a very

limited view of the moderator face (effectively 25%) and be bathed by the divergent penumbra from the LAD collimation. The beam to ITS will be trimmed using sintered B_4C just upstream of the monitor and sample to match the sample size - up to a maximum determined by the extent of the penumbra, but probably not exceeding the detector dimensions.

c) <u>Detector</u>

From Equation (3) it is clear that (L_i+L_f) should be as large as possible for the best energy resolution, the limitation imposed by keeping within the experimental hall gives $L_i+L_f \simeq 18.5$ m. The cororally to that statement is that the count rate at the detector will fall. Part of this loss can be regained by increasing the detector efficiency and also its area, subject to the need to discriminate against the detection of neutrons scattered by the sample into low angles. This latter point also requires that L_f be kept as large as practible, in this case $L_f = 4$ m. A possible detector would consist of eight 10 x 20 mm scintillator elements arranged to give a nominal overall area of 40 x 40 mm; its efficiency at $E = 1$ eV would be 50%. The use of a scintillation detector and fast electronics is necessary given the peak count rates likely to be encountered. Each scintillator element would be separately encoded.

A fast time-sorted monitor is an essential component in any attempt to use the pulsed neutron beam downstream of another instrument. A Li-glass beam-sampling monitor [19] will be well suited to the task.

d) <u>Instrument performance</u>

For $(L_i+L_f) = 18.5$ m, and using a 3 mm active thickness scintillation detector, the term $\Delta L/L$ in equation (3) becomes very small and the resolution is dominated by the term $\Delta t/t$. If it is further assumed that narrow t-o-f bins are used (e.g. 0.25 µs wide at the short times corresponding to $E \sim 10 - 20$ eV, and widening no faster than $\sim 1/t$), then the equation may be approximated by

$$\frac{\Delta E}{E} = \frac{2 \, \Delta\lambda}{\lambda} \simeq \frac{2 \, \Delta t_m}{t} \tag{9}$$

- 11 -

where Δt_m is the width, at a given energy, of the neutron pulse at the moderator face [20]. At energies $E > 0.1$ eV the relative energy resolution is $\Delta E/E \sim 0.28\%$; the resolution deteriorates for energies down to 10 meV where $\Delta E/E \sim 0.44\%$.

A nominal sample-out count rate is given by equation (3). Assuming the maximum LAD beam aperture such that ITS detector effectively views $\sim 25\%$ of the moderator face, a detector efficiency of 50% at $E = 1$ eV, and full intensity ISIS CH_4 moderator parameters [21], the predicted count rates (per second per t-o-f bin, Δt_D) are given in the following table:

E(eV)	0.01	0.1	1	10	
Δt_D (μs)	5	1.5	0.5	0.25	
I(E)	3.5	4.1	2.6	1.5	x 1000

Running the instrument downstream of LAD is clearly not without potential difficulty and some degree of liaison will be necessary — with LAD assuming the dominant role. For instance, it will not be possible to undertake precise measurements whenever the LAD sample has a strong resonance or exhibits a great deal of inelastic scattering (i.e. moderates the beam, as would a hydrogenous sample).

4. CONCLUSION

This report has attempted to show that transmittance measurements on a pulsed neutron source can be of significant benefit in many areas of science and technology. An outline design study has been presented of an intense transmission spectrometer (ITS) in which use is made of the existing LAD beamline by relocating the beamdump and installing the rather simple ITS components. The proposed high count rate, high resolution instrument therefore provides a useful addition to the present suite of ISIS instruments at minimum cost and without the need for a dedicated beam.

FIGURE CAPTIONS

1. A schematic diagram of the generic pulsed source transmission
    spectrometer.

2. a) The total correlation function for SiO_2 from a pulsed source
    transmission measurement (solid line) compared to that from a
    conventional 2-axis diffraction experiment [9]
    b) The total scattering cross section of SiO_2 together with the
    coherent bound (.....) and free-atom (-----) cross sections [9].

3. The total neutron cross section for iron; the edges are labelled as
    $n = h^2 + k^2 + l^2$ [11].

4. a) The cross section per hydrogen atom in $ZrH_{1.5}$; the theoretical
    (isotropic scattering) curve [12] corrected for thermal motions is
    also shown (-----) [13]
    b) The cross section for hydrogen in yttrium hydride [13].

5. The 22°C/735°C intensity ratio for the 1.098 eV resonance due to
    Hf-177 [16].

6. General layout of the LAD/ITS beamline.

7. Diagramatic section through the LAD/ITS beamline.

REFERENCES

1. C G Windsor, "Pulsed Neutron Scattering" (Taylor and Francis, London) 1982.

2. M C Moxon, J D Downes and D A J Endocott, AERE Harwell report AERE-R 8409, 1976.

3. A Clare, private communication.

4. S F Mughabghab, M Divadeenam and N E Holden, "Neutron Cross Sections" Vol 1 (Academic Press, New York) 1981.

5. L C W Hobbis, G H Rees and G C Stirling (editors) Rutherford Appleton Laboratory report RL-77-064/C 1977.

6. A C Wright, J Non Cryst Sol 76, 187, 1985.

7. G E Bacon, "Neutron Diffraction", 3 edition (Clarendon Press, Oxford) 1975.

8. R J Breen, R M Delaney, P J Persiani and A H Weber, Phys Rev 105, 517, 1957.

9. R N Sinclair and A C Wright, J Non Cryst Sol 57, 447, 1983.

10. E W J Mitchell and R J Stewart, Phil Mag 15, 617, 1967.

11. R G Johnson and C D Bowman, "Neutron Scattering 1981" AIP Conference Proceedings 89, 53, 1982.

12. E Fermi, Ricerca Sci 7, 13, 1936.

13. W L Whittemore and A W Reynolds, Phys Rev 113, 806, 1957.

14. J Eckert, T O Brun, A J Dianoux, J Howard, J J Rush and J W White, Proc "Scientific Opportunities with Advanced Facilities for Neutron Scattering" (Shelter Island) ed. G J Lander and V J Emery, US National Information Centre report CONF-8410256, 1984; and Los Alamos National Laboratory report LA-UR 85-783, 1985.

15. M C Moxon, "REFIT-A least squares program for resonance analysis of neutron transmission and capture data", AERE report NPLAP-UG1, March 1985.

16. P H Fowler, Proc ICANS VIII, Rutherford Appleton Laboratory report RAL-85-110, 138, 1985.

17. A Foderaro, "The Elements of Neutron Interaction Theory" (MIT Press) 1971.

18. V T Pugh and B W Hendy, Proc ICANS VIII, Rutherford Appleton Laboratory report RAL-85-110, 670, 1985.

19. P L Davidson, Rutherford Appleton Laboratory report RAL-85-032, 1985.

20. A D Taylor, Rutherford Appleton Laboratory report RAL-84-120, 1984.

21. T G Perring, A D Taylor and D R Perry, Rutherford Appleton Laboratory report RAL-85-029, 1985.
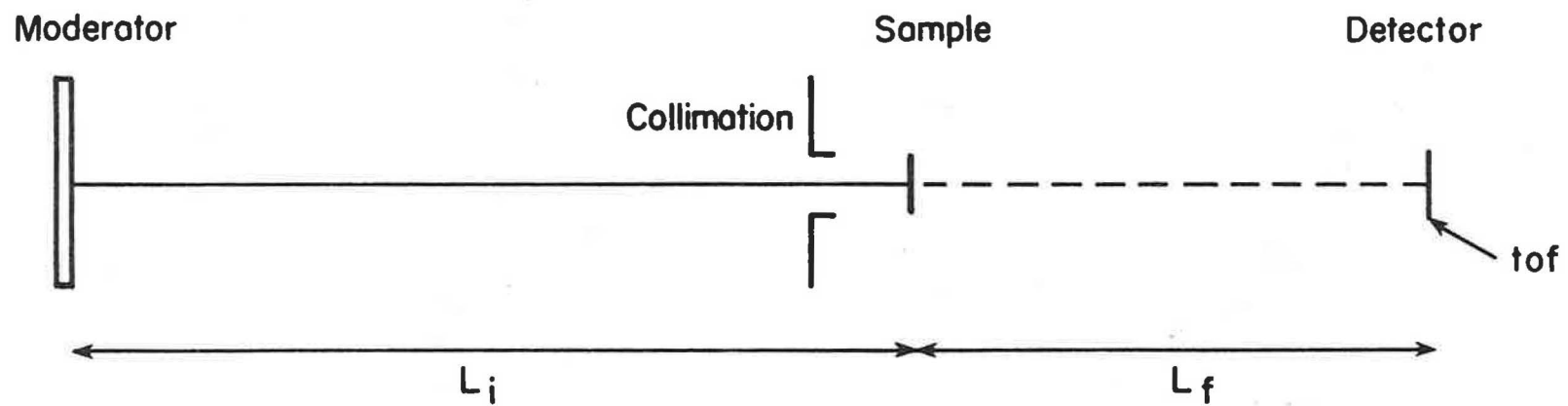
Figure 1   A schematic diagram of the generic pulsed source transmission spectrometer
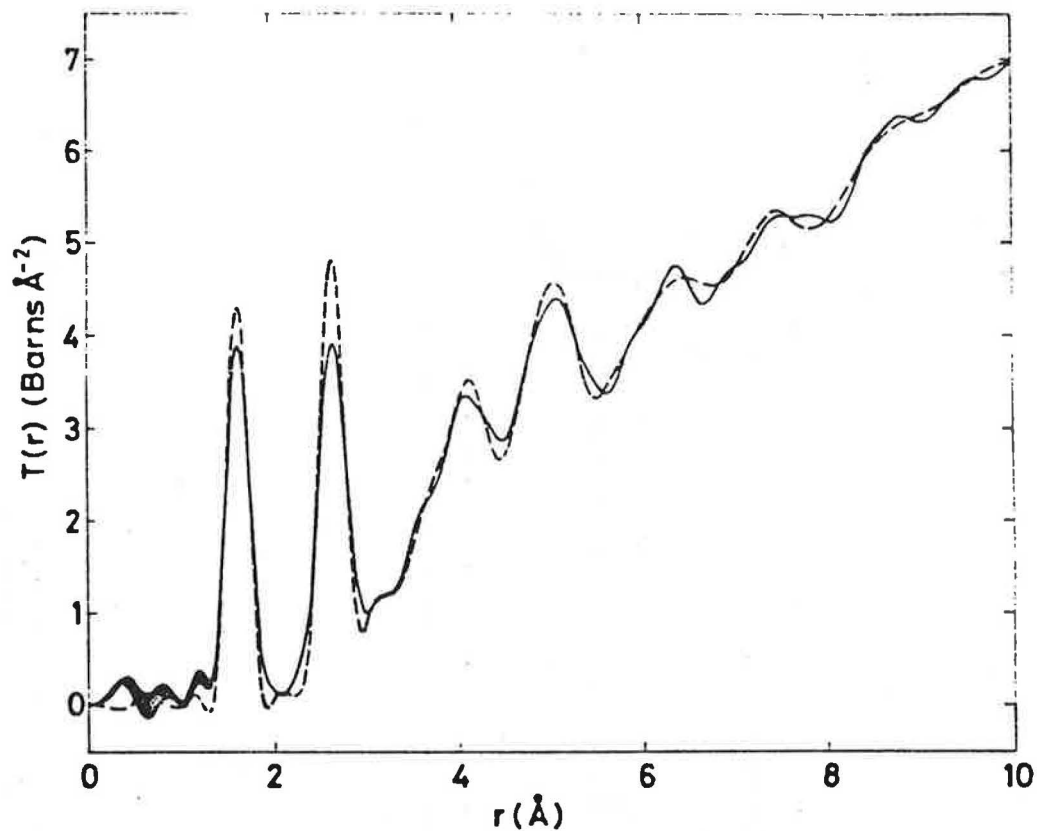
(a)
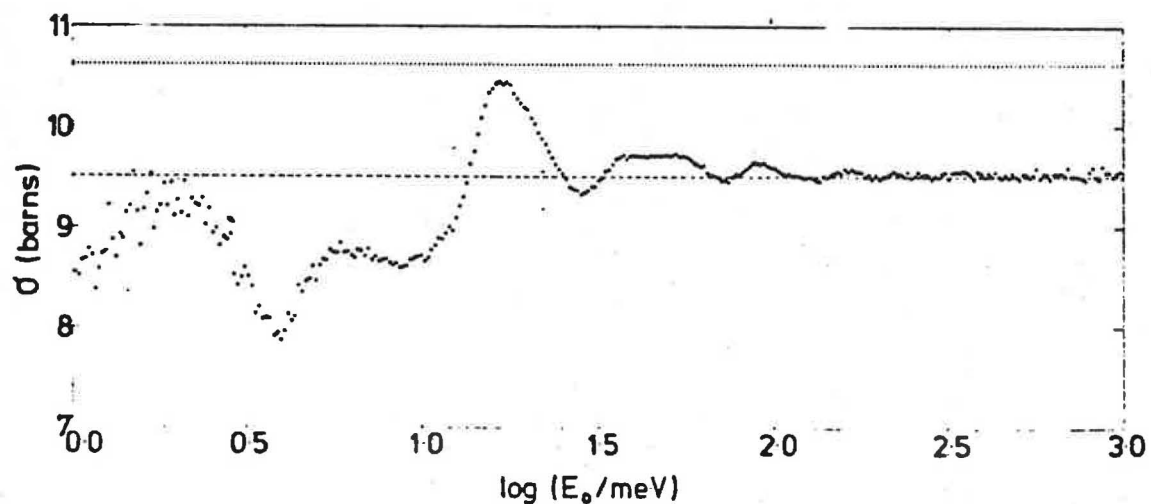
(b)

Figure 2. a) The total correlation function for SiO_2 from a pulsed
source transmission measurement (solid line) compared to
that from a conventional 2-axis diffraction experiment [9]
b) The total scattering cross section of SiO_2 together
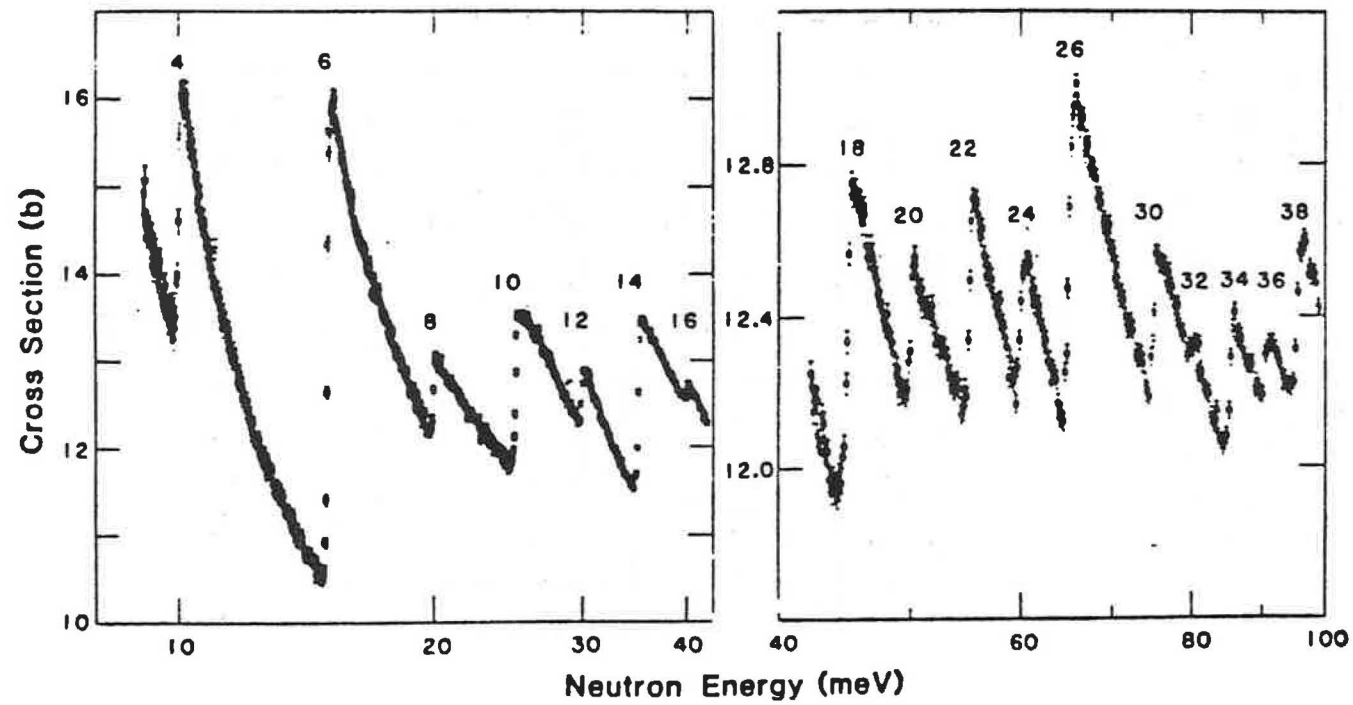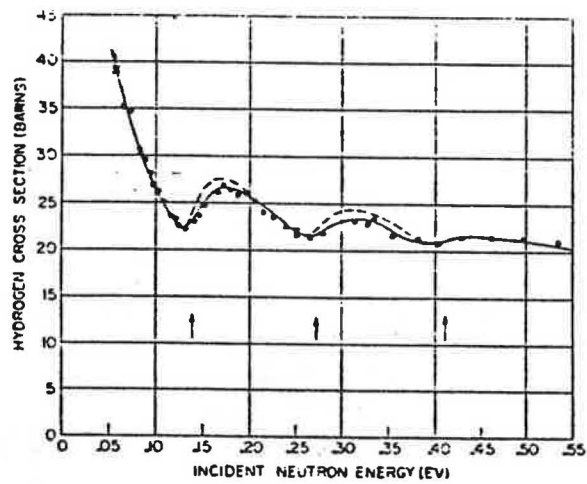with the coherent bound (.....) and free-atom (-----) cross
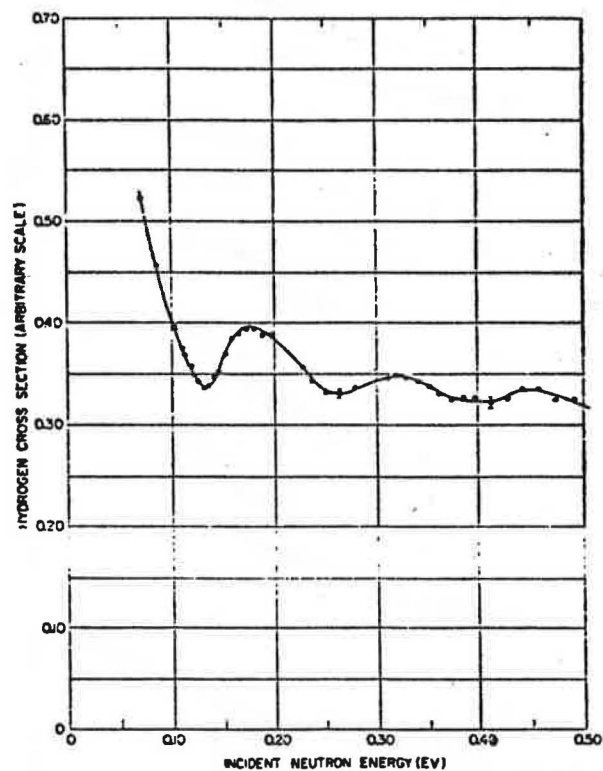sections [9].

Figure 3. The total neutron cross section for iron; the edges are labelled as $n=h^2 + k^2 + l^2$ [11].

(a)

(b)

Figure 4. a) The cross section per hydrogen atom in ZrH$_{1.5}$;
the theoretical (isotropic scattering) curve [12]
corrected for thermal motions is also shown (-----) [13]
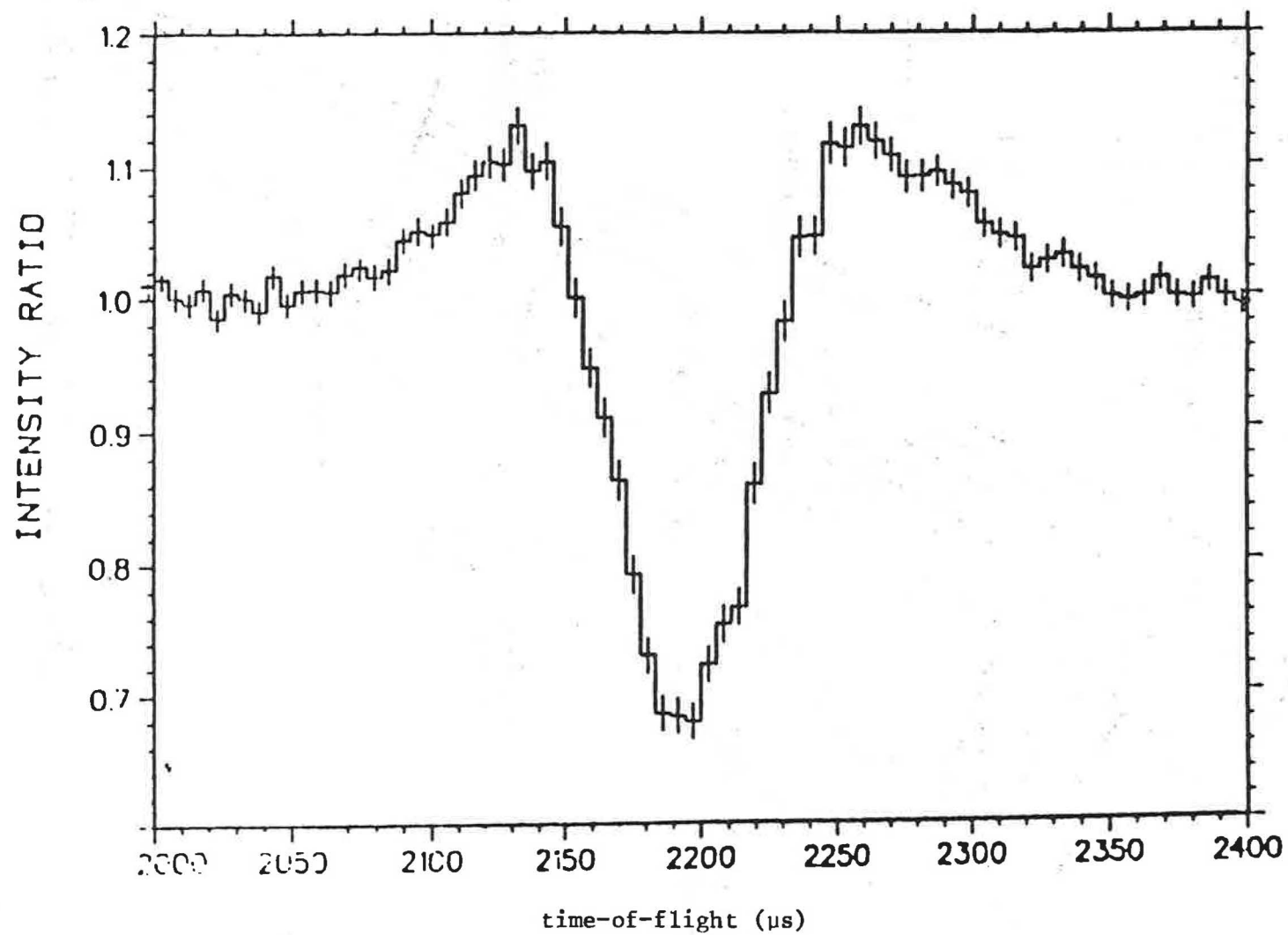b) The cross section for hydrogen in yttrium hydride [13].

Figure 5. The 22°C/735°C intensity ratio for the 1.098 eV resonance due to Hf-177 [16].
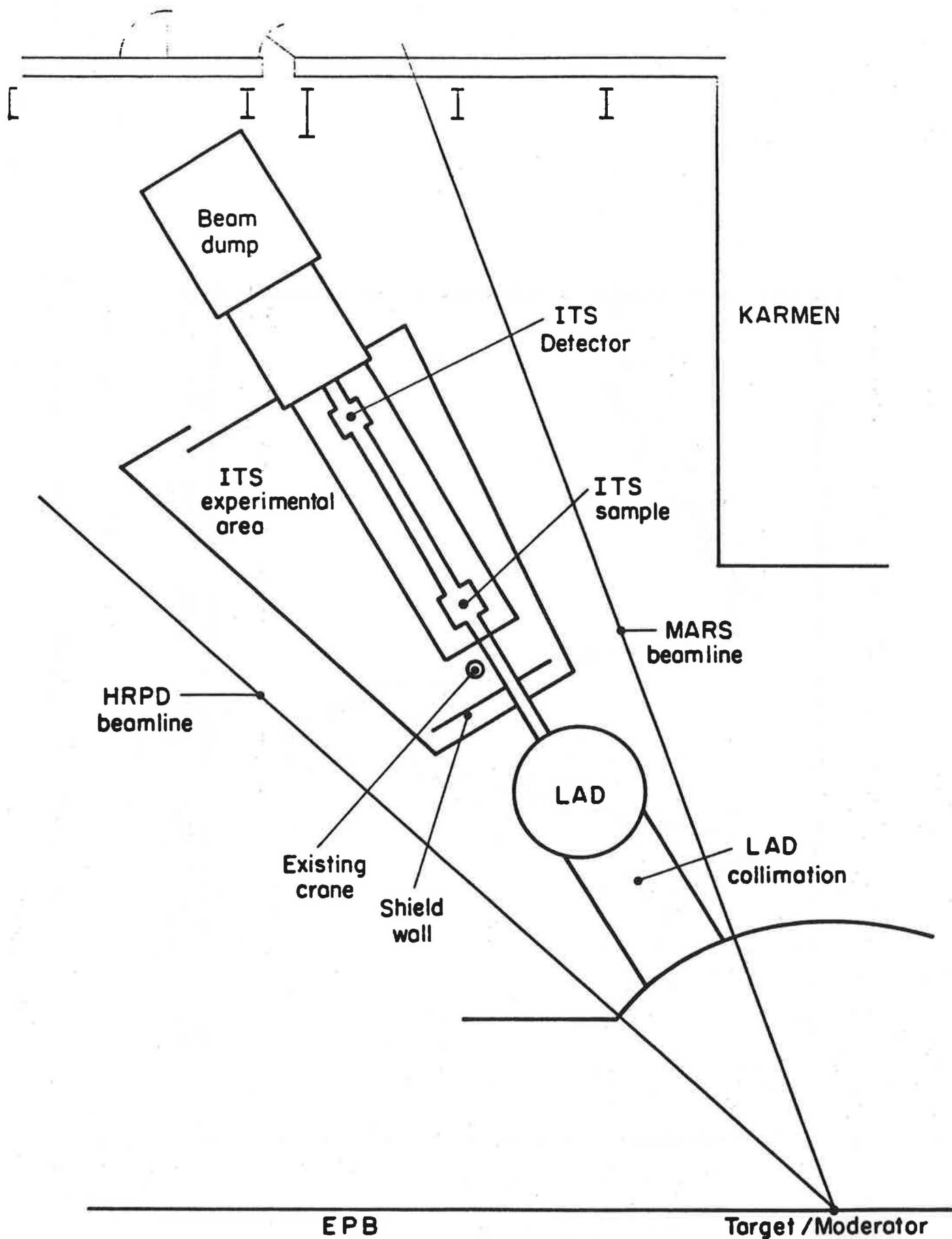
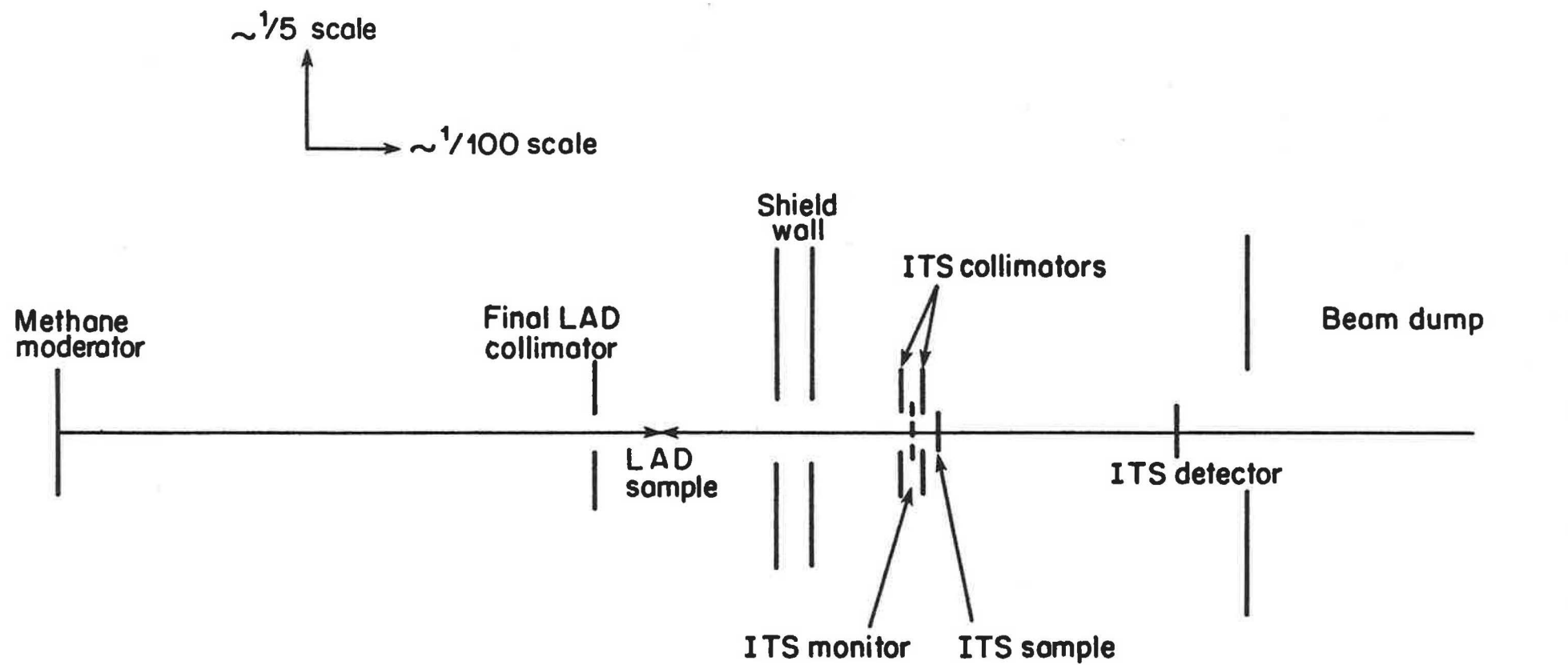**Figure 6**   General layout of the LAD/ITS beamline.

$\sim\frac{1}{5}$ scale

$\sim\frac{1}{100}$ scale

Shield wall

ITS collimators

Methane moderator

Final LAD collimator

Beam dump

LAD sample

ITS detector

ITS monitor   ITS sample

Figure 7   Diagramatic section through the LAD/ITS beamline.